Convergence of energy-differential ionization cross sections obtained from a *T*-matrix approach with *R*-matrix wave functions

K. Bartschat,[1] M. P. Scott,[2] P. G. Burke,[2] T. Stitt,[3] N. S. Scott,[3] A. N. Grum-Grzhimailo,[4] S. Riordan,[1] G. Ver Steeg,[1] and S. I. Strakhova[4]

[1]*Department of Physics and Astronomy, Drake University, Des Moines, Iowa 50311*

[2]*Department of Applied Mathematics and Theoretical Physics, The Queen's University of Belfast, Belfast BT7 1NN, Northern Ireland*

[3]*Department of Computer Science, The Queen's University of Belfast, Belfast BT7 1NN, Northern Ireland*

[4]*Institute of Nuclear Physics, Moscow State University, Mosco 119992, Russia*

(Received 7 February 2002; revised manuscript received 9 April 2002; published 17 June 2002)

The *T*-matrix approach, as formulated by Pindzola *et al.* [Phys. Rev. A **62**, 062718 (2000)] for calculating the single-differential ionization cross section (SDCS) has been further investigated. Using the ''intermediate-energy *R*-matrix method'' to obtain the full scattering wave function needed in the matrix element, we performed several case studies for the Temkin-Poet *S*-wave model of *e*-H scattering to study the dependence of the results on the box radius and the number of states included. Despite encouraging results before reaching convergence, we conclude that the method will ultimately not yield the correct form of the SDCS but instead will still suffer from unphysical oscillations.

DOI: 10.1103/PhysRevA.65.062715 PACS number(s): 34.80.Dp

I. INTRODUCTION

In recent years, the Temkin-Poet (TP) model problem [1,2] has been studied in great detail to investigate a simplified version of the classic three-body Coulomb break-up problem, namely electron-impact ionization of atomic hydrogen. In this model, only the *S* wave is considered and hydrogenic states with angular momentum $L=0$ are accounted for. It is important to note that this problem contains most of the difficulties associated with the full problem, but because of the restriction in angular momentum, it is now possible to push numerical methods essentially to convergence. Consequently, if the problem is formulated correctly and sufficient computational resources are allocated, one may expect numerical convergence to the ''physical'' answer for this simplified model.

A milestone regarding the convergence of numerical treatments was achieved in the pioneering work of Bray and Stelbovics [3], who developed the so-called ''convergent close-coupling'' (CCC) method. The essential idea of the method is the extension of the standard discrete-state-only close-coupling method through inclusion of a large number of square-integrable pseudo-states. While formulated in momentum-space, the CCC method is closely related to earlier pseudo-state approaches [4,5], which were not necessarily pushed to convergence in all aspects due to the limited computational resources at the time, and particularly to the *R*-matrix with pseudo-states (RMPS) method [6,7]. Another close relative of the CCC method is the intermediate-energy *R*-matrix (IERM) approach [8,9], which has been shown to yield essentially identical results to CCC and RMPS [10,11] if all three methods are driven to convergence. Without attempting completeness, we also mention some of the many other methods used for both the TP and the full $e-$H collision problem, namely the eigenchannel *R*-matrix [12], hyperspherical close-coupling [13,14], the *J*-matrix method [15], exterior complex scaling (ECS) [16], direct finite-difference methods (FDM) [17,18], and time-dependent wave-packet approaches [19–21]. Overall, it was found that the total excitation and ionization cross sections could be predicted with very high accuracy by essentially all of these methods, with the only practical limitation being the available computational resources. The complete problem, however, for the present case is the distribution of the excess energy among the two outgoing electrons. It is determined by the single-differential (with respect to the energy loss) cross section (SDCS). Interestingly, this SDCS could only be obtained in a straightforward manner by methods that either matched to exact boundary conditions or did not rely on boundary conditions at all in the extraction procedure.

Finally, of particular interest for the present work is the *T*-matrix method suggested by Pindzola, Mitnik, and Robicheaux [22]. They addressed the problem of the unphysical asymmetry in the SDCS with respect to half of the available energy for the two outgoing electrons, found in the standard CCC, RMPS, and IERM results. The reason for this asymmetry has been discussed in great detail [23–26]; it is effectively due to the unequal treatment of the two positive-energy electrons. For further discussion, particularly with respect to the way the SDCS is extracted from a numerical wave function, see also the work by Rescigno *et al.* [27] and by Madison *et al.* [28]. However, Pindzola *et al.* [22] showed how the asymmetry can be removed by using a *T*-matrix formulation to extract the ionization amplitude and, consequently, the SDCS. In this formulation, the ionization amplitude for the TP model (in atomic units) is defined as

$$f(k_2,k_1,k_0)=\int_0^\infty dr_1\int_0^\infty dr_2 C(k_1,r_1) \times C(k_2,r_2)\frac{1}{r_>}\Psi_0^+(r_1,r_2), \qquad (1)$$

where k_0 is the linear momentum of the incident electron while k_1 and k_2 are the momenta of the two outgoing elec-

trons in the final state. [Only the magnitudes of the momenta matter in the TP model.] Furthermore, $1/r_>$ with $r_> = \max(r_1,r_2)$ is the interaction potential, $C(k,r)$ is a Coulomb wave for an electron with momentum k, and $\Psi_0^+(r_1,r_2)$ is the full solution of the collision problem. The boundary conditions for $\Psi_0^+(r_1,r_2)$ must be chosen in such a way that there is an incoming plane wave in the channel with the target in the $1s$ initial state, and outgoing waves in all collision channels (including the elastic one). Assuming that $\Psi_0^+(r_1,r_2)$ is properly antisymmetrized, one sees immediately that the above scheme is explicitly symmetric against interchanging the two outgoing electrons in the calculation of the SDCS given by

$$\frac{d\sigma}{d\epsilon} \equiv \frac{8}{k_0^2}|f(k_2,k_1,k_0)|^2, \tag{2}$$

where ϵ is the energy of the ejected electron. Equation (2) is consistent with the conventions of Pindzola *et al.* [22], except that all continuum functions for energy $k^2/2$ are assumed to behave as $k^{-1/2}$ times a sine function in the asymptotic regime.

The initial tests performed by Pindzola *et al.* [22] using the above formulation were quite promising, although some oscillations in the SDCS results were found even in their largest RMPS calculations. However, they attributed these oscillations to the finite mesh size and the limited number of states included in the close-coupling expansion, and therefore expressed optimism that these problems could be resolved in a more or less straightforward manner. Of course, it is known that the wave function $\Psi_0^+(r_1,r_2)$, if calculated by the RMPS or similar methods, is asymptotically not correct due to the finite range of the pseudo-orbitals. Although this problem might be more obvious in the ''prior form'' of Eq. (1), where the full scattering wave function $\Psi_f^-(r_1,r_2)$ is needed on the left-hand-side of the matrix element while the right-hand-side is a simple product of the initial target state and a plane wave for the projectile, it exists in the above ''post'' form as well, since $\Psi_0^+(r_1,r_2)$ should really contain two outgoing Coulomb-type waves in the ionization channels.

The present work was therefore motivated by the question of whether or not the results from the above T-matrix method would ultimately converge to the correct answer or whether problems, particularly oscillations, might still persist. We also note that highly accurate results for this particular problem have recently become available [18,29]. Because of its numerical stability when a very large number of pseudo-states are included in the close-coupling expansion, we decided to calculate the wave function $\Psi_0^+(r_1,r_2)$ using the IERM method. The basic ideas behind this method and the construction of $\Psi_0^+(r_1,r_2)$ from the standard IERM output are summarized in the next section, followed by the discussion of our results and some concluding remarks.

II. THE IERM METHOD

The R-matrix method, in general, proceeds by partitioning configuration space into two regions by a sphere of radius $r=a$, where r is the relative coordinate of the scattering electron and the center of gravity of the target atom or ion. This sphere is chosen to completely envelope the electronic orbitals of the target atom or ion. Hence in the internal region ($r \leqslant a$) exchange and correlation effects between the scattering electron and the target electrons must be included, whereas in the external region exchange effects can be neglected and the problem simplifies considerably.

In the internal region the $(N+1)$-electron wave function at energy E is expanded in terms of an energy-independent basis set, ψ_k, as

$$\Psi_E = \sum_k A_{Ek}\psi_k . \tag{3}$$

The basis states, ψ_k, are expanded in the form

$$\begin{aligned}\psi_k(\mathbf{x}_1,\ldots,\mathbf{x}_{N+1}) = \mathcal{A}\sum_{ij} & \tilde{\Phi}_i(\mathbf{x}_1,\ldots,\mathbf{x}_N;\hat{\mathbf{r}}_{N+1}\sigma_{N+1}) \\ & \times r_{N+1}^{-1}u_{ij}(r_{N+1})c_{ijk} \\ & + \sum_j \chi_j(\mathbf{x}_1,\ldots,\mathbf{x}_{N+1})d_{jk},\end{aligned} \tag{4}$$

where the channel functions $\tilde{\Phi}_i$ are obtained by coupling the orbital and spin angular momenta of the target states Φ_i with those of the scattered electron to form eigenstates of the total orbital and spin angular momenta L and S, their z-components M_L and M_S, and the parity π. The set of states Φ_i will include target eigenstates and pseudo-states to allow for the effect of the infinite number of highly excited bound states and continuum states of the target atom or ion which cannot be explicitly included in the calculation. The u_{ij} are members of a complete set of numerical orbitals used to describe the radial motion of the scattered electron and the χ_j are $(N+1)$-electron configurations included to allow for short range correlation effects between the scattered and target electrons. The coefficients c_{ijk} and d_{ij} are obtained by diagonalizing the $(N+1)$-electron Hamiltonian matrix in the internal region.

Each of the target eigenstates and pseudo-states is expanded in terms of a sum of orthonormal configurations

$$\Phi_i(\mathbf{x}_1,\ldots,\mathbf{x}_N) = \sum_j \phi_j(\mathbf{x}_1,\ldots,\mathbf{x}_N)c_{ij}, \tag{5}$$

where the ϕ_j are constructed from a set of orthonormal one-electron orbitals which can be either bound physical orbitals or pseudo-orbitals, included to represent electron correlation effects or to represent the target continuum.

In the IERM method, the bound orbitals and the pseudo-orbitals are members of the same numerical continuum basis which is used to describe the motion of the scattered electron. For the TP-model (zero angular momentum only), the radial functions of these orbitals are solutions of the differential equation

$$\left(\frac{d^2}{dr^2}+\frac{2Z}{r}+k_n^2\right)u_n(r)=0, \tag{6}$$

subject to the boundary conditions

$$u_n(0)=0,$$

$$\frac{a}{u_n(a)}\frac{du_n(r)}{dr}\bigg|_{r=a}=b, \tag{7}$$

where b is a constant, usually taken as zero. The IERM basis produced from these functions is a more densely packed pseudo-state basis, with respect to the target state energy levels, than a typical RMPS pseudo-state basis [30]. It depends, however, on the R-matrix boundary, with the density increasing with increasing radius. It is therefore very appropriate in the study of scattering processes such as electron-impact ionization close to threshold [11,30]. In the calculation with a box radius of $400a_0$, for example, from which results are shown below for an incident energy of 20 eV, 95 S states were included in the close-coupling expansion. Of those 95 states, the lowest 12 represented very good approximations to the physical discrete states, the next 6 still had negative energy and therefore represented coupling to the remaining members of the discrete spectrum, and the other 77 states represented the ionization continuum. For an incident electron energy of 20 eV, 72 of these continuum states represented open channels while the remaining 5 were closed. The ability to include this very large number of pseudo-states (and more if desired) without running into linear-dependence problems is the major strength of the IERM approach.

Finally, it is necessary to construct the wave function $\Psi_0^+(r_1,r_2)$ using the IERM basis. We first express $\Psi_0^+(r_1,r_2)$ in terms of the energy-independent R-matrix basis states, ψ_k, as in Eq. (3)

$$\Psi_0^+(r_1,r_2)=\sum_k A_{Ek}\psi_k, \tag{8}$$

where A_{Ek} are complex coefficients and E is the total energy of the two-electron system. Asymptotically, we construct the wave function $\Psi_0^+(r_1,r_2)$ to correspond to a plane wave in the incident channel together with spherical outgoing waves in all scattering channels. For outgoing wave boundary conditions, the coefficients A_{Ek} are given by [31]

$$A_{Ek}=\frac{1}{2a(E_k-E)}\sum_i w_{ik}(a)\left(a\frac{dy_{ip}}{dr}-by_{ip}\right)_{r=a}, \tag{9}$$

where the surface amplitudes $w_{ik}(a)$ are defined in terms of the radial basis functions $u_{ij}(a)$ on the R-matrix boundary by

$$w_{ik}(a)=\sum_i c_{ijk}u_{ij}(a). \tag{10}$$

In the present IERM calculation, the u_{ij} will be members of the basis set defined by Eqs. (6) and (7). The radial functions, $y_{ip}(r)$, in Eq. (9) behave asymptotically as

$$y_{ip}(r)\underset{r\to\infty}{\sim}k_i^{-1/2}(e^{-i\theta_i}\delta_{ip}-e^{i\theta_i}S_{ip}), \tag{11}$$

where S_{ip} is the scattering matrix, $\theta_i=k_ir$ for the TP model, and $p=1$ for scattering from the ground state. (As mentioned above, however, this standard choice is problematic for the ionization channels.) We note that $y_{ip}(a)$ is related to its derivative on the R-matrix boundary, $r=a$, through the R-matrix

$$y_{ip}(a)=\sum_j R_{ij}\left(a\frac{dy_{jp}}{dr}-by_{jp}\right)_{r=a}, \tag{12}$$

where the R-matrix at energy E is given by

$$R_{ij}=\frac{1}{2a}\sum_k\frac{w_{ik}(a)w_{jk}(a)}{E_k-E}+R_{ij}^{\rm corr}\delta_{ij}. \tag{13}$$

$R_{ij}^{\rm corr}\delta_{ij}$ is the usual Buttle correction to the diagonal elements of the R-matrix [32]. The expansion coefficients A_{Ek} can then be written in matrix form as

$$\mathbf{A}(E)=\mathbf{G}\cdot\mathbf{w^T}\cdot\mathbf{R^{-1}}\cdot\mathbf{y^+}, \tag{14}$$

where we have omitted the p index for simplicity. The matrix $\mathbf{G}$ is a diagonal matrix with elements

$$G_{kk}=\frac{1}{2a(E_k-E)}. \tag{15}$$

All the quantities in Eq. (14) are real except for $\mathbf{y^+}$, which satisfies the complex boundary conditions (11). For convenience, $\mathbf{y^+}$ can be written in terms of the real solutions

$$F_{ij}(r)\underset{r\to\infty}{\sim}k_i^{-1/2}(\sin\theta_i\delta_{ij}+\cos\theta_iK_{ij}),\quad\text{open channels;}$$

$$F_{ij}(r)\underset{r\to\infty}{\sim}\exp(-|k_i|r)\delta_{ij},\quad\text{closed channels.} \tag{16}$$

We then find that

$$\mathrm{Re}\,\mathbf{y^+}=2\mathbf{F}\cdot\mathbf{K}(\mathbf{1}+\mathbf{K}^2)^{-1}, \tag{17}$$

$$\mathrm{Im}\,\mathbf{y^+}=-2\mathbf{F}\cdot(\mathbf{1}+\mathbf{K}^2)^{-1}. \tag{18}$$

In the current IERM calculation, the R-matrix boundary is taken sufficiently large so that Eq. (16) is satisfied at $r=a$. The K-matrix, $\mathbf{K}$, can then be extracted by matching radial solutions for the scattered electron on the R-matrix boundary in the usual way (see, e.g. [33]). Knowing the expansion coefficients c_{ijk} and d_{jk} from the diagonalization of the two-electron Hamiltonian matrix in the internal region, we can construct the R-matrix basis states, ψ_k, and hence complete the determination of the wave function $\Psi_0^+(r_1,r_2)$.

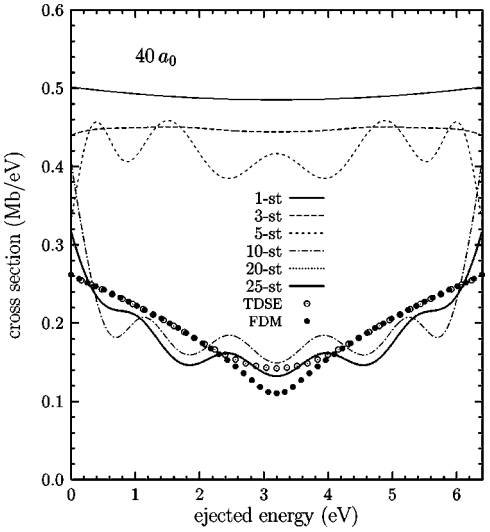

FIG. 1. Energy-differential ionization cross section for the singlet spin channel of the Temkin-Poet model at an incident energy of 20 eV, obtained as for a fixed *R*-matrix radius of $40a_0$ as a function of the number of target states used in the close-coupling expansion. Note that the results for 20 and 25 states are indistinguishable within the thickness of the respective lines. Also shown are recent results from time-dependent (TDSE) [21] and finite-difference (FDM) methods [29].

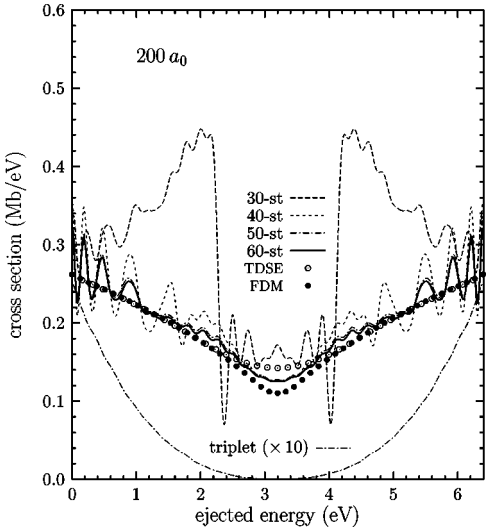

FIG. 2. Same as Fig. 1 for a radius of $200a_0$. Also shown are the results from the 50-state calculation for the triplet spin channel (multiplied by 10 with the spin factor of 3/4 included).

III. RESULTS AND DISCUSSION

For direct comparison with the results of Pindzola *et al.* [22], we also performed our case studies for an incident energy of 20 eV. Figure 1 displays our first set of results, namely for a box size of $40a_0$. This relatively small box can essentially accommodate the physical bound orbitals $1s$, $2s$, and $3s$, and hence the very good agreement between our 1-state and 3-state results and those shown in Fig. 3 of Pindzola *et al.* [22] (for a box size of $50a_0$) is not surprising but serves as a valuable check of the numerical procedure. Since the 5-state model includes two pseudo-states that are constructed with the same philosophy but a different boundary condition compared to the RMPS method, we now expect similar though not identical results from the IERM and RMPS methods. This is indeed the case, as seen from a comparison of the two figures mentioned above. Most importantly, however, we see that the curves for 20 and 25 states included in the close-coupling expansion are essentially indistinguishable on the graph. We therefore conclude that this particular model (for a box radius of $40a_0$) is converged with respect to the number of states.

Also shown in Fig. 1 is the result of our recent time-dependent calculation [21] that was pushed to a radius of $480a_0$. Comparison with the FDM results of Jones and Stelbovics [29] shows that these results are close to the exact answer, except near the equal-energy sharing case, where the width of the Gauss package and a very slow convergence with the box radius causes the minimum to smear out. Since the oscillations of the *T*-matrix results around the TDSE and FDM predictions are apparently not removable by including more states in the close-coupling expansion, we conclude that these oscillations are an artifact of the boundary conditions imposed on $\Psi_0^+(r_1,r_2)$ by the present IERM approach, which are (like those in the RMPS formulation) inappropriate for the ionization problem.

Figure 2 shows the corresponding results for a box radius of $200a_0$. Here the 30-state calculation corresponds to the case where already more than 20 pseudo-states are included in the calculation, but the highest pseudo-state energy is only 2.2 eV, i.e., 15.8 eV above the elastic threshold. As a result, the predictions from this particular model are far away from the correct answer and show a strange pattern near the equal-energy sharing situation. Nevertheless, one could actually argue that the individual points are still ''better'' (namely lower) than what would be obtained in 1-state and 3-state models. The other calculations, including 40, 50, and 60 states, respectively, provide significantly improved answers. In these cases, pseudo-states with energies up to 4.5, 7.4, and 11.0 eV, respectively, were included in the calculations. From the nearly identical results obtained in the 50-state and 60-state models, we conclude that convergence with respect to the number of states is essentially reached once a few closed channels are included in the calculation. Note, however, that even after reaching this convergence the oscillations in the SDCS persist. We also point out that the amplitude of the oscillations in the asymmetric energy-sharing situation ($\epsilon \ll E_{\max} - \epsilon$) is not decreasing considerably compared to the smaller box radius (see Fig. 1). Finally, we investigated the triplet spin channel for this box size. As seen by the results from the 50-state model, oscillations are essentially negligible in this case. This finding agrees with those from studies using some of the other methods mentioned above.

Figure 3 shows the behavior of our results from converged (with respect to the number of states) calculations as a function of the box radius. Although the results for $300a_0$ and $400a_0$ are quite similar, thereby indicating convergence with respect to the box radius as well, these results are apparently not physical. The amplitudes of the oscillation near the edges (i.e., for highly asymmetric energy sharing) are

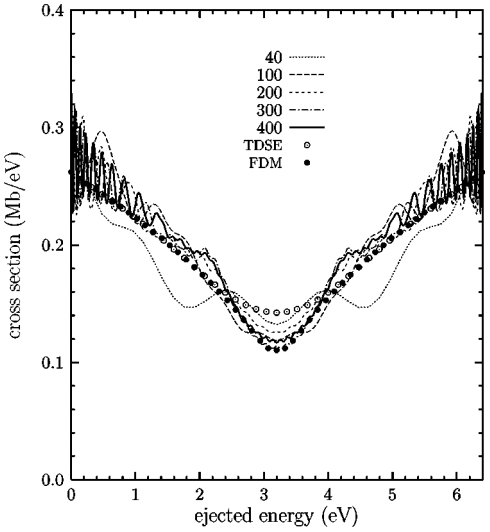

FIG. 3. Energy-differential ionization cross section for the singlet spin channel of the Temkin-Poet model at an incident energy of 20 eV, obtained for different values of the *R*-matrix radius. The calculations are converged with the number of states included in the close-coupling expansion. Also shown are recent results from time-dependent (TDSE) [21] and finite-difference (FDM) methods [29].

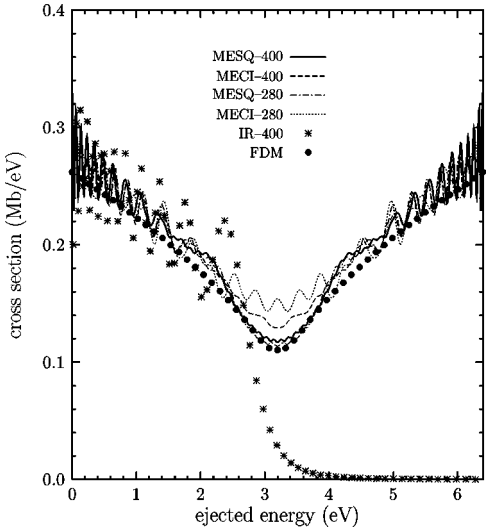

FIG. 4. Energy-differential ionization cross section for the singlet spin channel of the Temkin-Poet model at an incident energy of 20 eV, obtained by performing the integration over the full square of side length $400a_0$ (MESQ–400), a quarter circle of radius $400a_0$ (MECI–400), and a reduced square (quarter circle) of side length (radius) $280a_0$ (MESQ–280 and MECI–280). In all cases, the wave function $\Psi_0^+(r_1,r_2)$ was constructed on the full square. Also shown are the SDCSs obtained from the integration-rule approach using the excitation cross sections for the various pseudo-states together with their energy separation, as well as the FDM result [29].

substantial, and we also note a ''shoulder'' just before entering the ''trough'' near the center. Around the equal-energy sharing regime, however, the *T*-matrix results are apparently superior even to the best TDSE data that we could generate with a comparable computational effort. Consequently, it may be worthwhile to investigate the possibility of combining the strengths of both methods in the respective energy-sharing regimes.

After plotting the actual wave function on the mesh, it seemed possible that the construction of the wave function near the end of the mesh might be the reason for some, if not all, of the problems. We therefore explored even more possibilities to extract the ionization cross section. An example is shown in Fig. 4, in which we compare the results obtained from calculations where the wave function $\Psi_0^+(r_1,r_2)$ was determined over the full rectangular (r_1,r_2) mesh reaching out to $400a_0$, but the radial integrations in Eq. (1) were performed over the full square $(0\leqslant r_1,r_2\leqslant 400a_0)$, a quarter circle $(r_1^2+r_2^2\leqslant 400a_0)$, a smaller square $(0\leqslant r_1,r_2\leqslant 280a_0)$, and a smaller quarter circle $(r_1^2+r_2^2\leqslant 280a_0)$. Obviously, the problem is not solved by either one of these prescriptions either.

However, it is worth noting that the oscillations in Fig. 4 are of smaller amplitude than what is obtained in the ''standard'' extraction of the SDCS from CCC, RMPS, and IERM calculations, where a trapezoidal-based integration rule is used to relate the excitation cross sections of the positive-energy pseudo-states to the SDCS [7]. Here the SDCS at a pseudo-state energy ϵ_i is simply approximated by the excitation cross section σ_i of this state divided by half the energy difference to the two neighboring states. Although our computational facilities did not allow for a *T*-matrix IERM calculation at bigger radii than $400a_0$, we used the two-dimensional *R*-matrix propagator approach [34] to perform a standard IERM calculation over even bigger ranges up to $800a_0$. As can be seen from Fig. 5, only the number but not the amplitude of the oscillations changes substantially in the ''integration-rule'' method when going from $400a_0$ to $800a_0$. It therefore seems unlikely that the oscillations will completely disappear in the *T*-matrix method even if the box

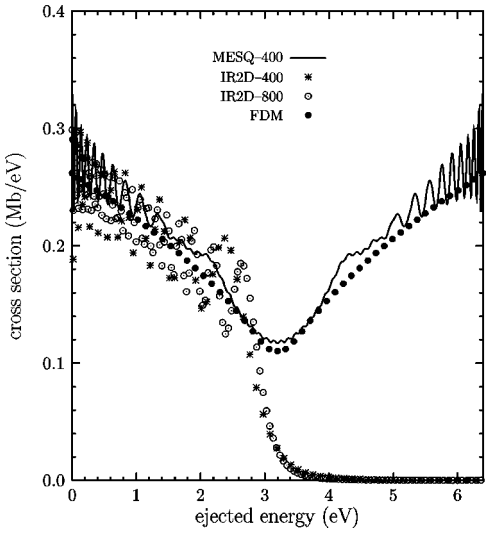

FIG. 5. Energy-differential ionization cross section for the singlet spin channel of the Temkin-Poet model at an incident energy of 20 eV, obtained by the *T*-matrix approach over a square of side length $400a_0$ (MESQ–400) and by integration-rule extractions of the SDCS from IERM calculations with box-sizes of $400a_0$ and $800a_0$, respectively.

radius is increased further. Nevertheless, partial success can be claimed from the fact that the amplitude of the oscillations is reduced when changing the procedure from the integration rule to the *T*-matrix approach. This, together with the built-in symmetry of the SDCS results around half the excess energy, might improve the confidence in smoothing procedures.

IV. SUMMARY AND CONCLUSIONS

We have used the IERM method, in combination with the *T*-matrix approach, to calculate the energy-differential ionization cross sections for the singlet channel of the TP model for an incident electron energy of 20 eV. For fixed box radii between $40a_0$ and $400a_0$, it was possible to include a sufficient number of states in the close-coupling expansion to ensure convergence with the number of coupled states. With their amplitude and location depending on the details of the integration procedure used in the *T*-matrix approach, unphysical oscillations around the correct answer still remained even in our largest calculations. Although we cannot rule out the possibility of convergence at a truly ''infinite'' mesh, indications are that the *T*-matrix method, as formulated above, will *not* remove all the unphysical oscillations in practical calculations. Although the results are symmetric (by construction) around the equal-energy sharing point and the oscillations exhibit a smaller amplitude than those seen in the standard integration-rule extraction procedure of the SDCS, it seems very likely that the consequences of imposing incorrect asymptotic boundary conditions on the full scattering wave function cannot be completely eliminated by this approach. Although this result may not be too surprising after all, we expect it to be very relevant in setting the directions for future work on this fundamental collision problem.

ACKNOWLEDGMENTS

We would like to thank Professor A. T. Stelbovics for providing unpublished FDM results at 20 eV. One of us (K.B.) appreciates stimulating discussions with Dr. B. I. Schneider regarding this problem. This work was supported, in part, by the United States National Science Foundation under Grant No. PHY-0088917 (K.B., S.R., and G.V.), by NATO under Grant No. PST.CLG.976837 (K.B., M.P.S., P.G.B., A.N.G., and S.I.S.), and by the EPSRC (P.G.B., M.P.S., and N.S.S.). One of us (T.S.) gratefully acknowledges the receipt of an ESF/Queen's University postgraduate studentship.

[1] A. Temkin, Phys. Rev. **126**, 130 (1962).
[2] R. Poet, J. Phys. B **11**, 3081 (1978).
[3] I. Bray and A.T. Stelbovics, Phys. Rev. Lett. **69**, 53 (1992).
[4] P.G. Burke and J.F.B. Mitchell, J. Phys. B **6**, 320 (1973).
[5] J. Callaway and D.H. Oza, Phys. Rev. A **29**, 2416 (1984).
[6] K. Bartschat, E.T. Hudson, M.P. Scott, P.G. Burke, and V.M. Burke, J. Phys. B **29**, 115 (1996).
[7] K. Bartschat and I. Bray, Phys. Rev. A **54**, R1002 (1996).
[8] P.G. Burke, C.J. Noble, and M.P. Scott, Proc. R. Soc. London, Ser. A **410**, 289 (1987).
[9] M. Le Dourneuf, J.M. Launay, and P.G. Burke, J. Phys. B **23**, L559 (1990).
[10] K. Bartschat, I. Bray, P.G. Burke, and M.P. Scott, J. Phys. B **29**, 5493 (1996).
[11] M.P. Scott, P.G. Burke, K. Bartschat, and I. Bray, J. Phys. B **30**, L309 (1997).
[12] K. Meyer, C.H. Greene, and I. Bray, Phys. Rev. A **52**, 1334 (1995).
[13] S. Watanabe, Y. Hosoda, and D. Kato, J. Phys. B **26**, L495 (1993).
[14] D. Kato and S. Watanabe, Phys. Rev. Lett. **74**, 2443 (1995).
[15] D.A. Konovalov and I.E. McCarthy, J. Phys. B **27**, L407 (1994).
[16] M. Baertschy, T.N. Rescigno, W.A. Isaacs, and C.W. McCurdy, Phys. Rev. A **60**, R13 (1999).
[17] Y.D. Wang and J. Callaway, Phys. Rev. A **50**, 2327 (1994).
[18] S. Jones and A.T. Stelbovics, Phys. Rev. Lett. **84**, 1878 (2000).
[19] W. Ihra, M. Draeger, G. Handke, and H. Friedrich, Phys. Rev. A **52**, 3752 (1995).
[20] F. Robicheaux, M.S. Pindzola, and D.R. Plante, Phys. Rev. A **55**, 3573 (1997).
[21] K. Bartschat, S. Riordan, and G. Ver Steeg, Phys. Rev. A **65**, 060701 (2002).
[22] M.S. Pindzola, D. Mitnik, and F. Robicheaux, Phys. Rev. A **62**, 062718 (2000).
[23] I. Bray, Phys. Rev. Lett. **78**, 4721 (1997).
[24] G. Bencze and C. Chandler, Phys. Rev. A **59**, 3129 (1999).
[25] I. Bray, Phys. Rev. A **59**, 3133 (1999).
[26] A.T. Stelbovics, Phys. Rev. Lett. **83**, 1570 (1999).
[27] T.N. Rescigno, C.W. McCurdy, W.A. Isaacs, and M. Baertschy, Phys. Rev. A **60**, 3740 (1999).
[28] D.H. Madison, D.O. Odero, and J.L. Peacher, J. Phys. B **33**, 4409 (2000).
[29] A.T. Stelbovics (private communication).
[30] M.P. Scott, T. Stitt, N.S. Scott, and P.G. Burke, in *Correlations, Polarizations, and Ionization in Atomic Systems*, edited by D.H. Madison and M. Schulz, AIP Conf. Proc. No. 604 (AIP, Melville, NY, 2002).
[31] K.L. Bell, P.G. Burke, and A.E. Kingston, J. Phys. B **10**, 3117 (1977).
[32] P.J.A. Buttle, Phys. Rev. **160**, 719 (1967).
[33] P.G. Burke, A. Hibbert, and W.D. Robb, J. Phys. B **4**, 153 (1971).
[34] T. Stitt, Ph.D. thesis, The Queen's University of Belfast, in preparation.